IOP Publishing Nanotechnology

Nanotechnology **25** (2014) 025705 (6pp) doi:10.1088/0957-4484/25/2/025705

Observation of localized strains on vertically grown single-walled carbon nanotube forests via polarized Raman spectroscopy

June Park[1], Kwang Heo[2], Seunghun Hong[2], Yo-Sep Min[3] and Maeng-Je Seong[1]

[1] Department of Physics, Chung-Ang University, Seoul, 156-756, Korea
[2] School of Physics and Astronomy, Seoul National University, Seoul, 151-747, Korea
[3] Department of Chemical Engineering, Konkuk University, Seoul, 143-701, Korea

E-mail: mseong@cau.ac.kr

Received 14 August 2013, in final form 21 October 2013
Published 12 December 2013

Abstract

Vertically grown single-walled carbon nanotube (V-SWCNT) forests, synthesized by water-assisted plasma-enhanced chemical vapor deposition, were studied using polarized micro-Raman spectroscopy. Among three different sections (root, center and end) along the vertical growth direction, the degree of V-SWCNT alignment was highest in the center section. Raman frequency red-shifts up to 7 and 13 cm^{-1}, for RBM and G-band, respectively, were observed in the center section, with respect to the Raman frequencies measured in the root and the end sections. Raman frequency downshift and concurrent linewidth broadening of the G-band, revealing a localized strain, were also observed in the center section. The existence of a localized strain in the center section of the V-SWCNT was further confirmed by observing a strong polarization anisotropy of up to 8 cm^{-1} in the G-band Raman frequency for different polarized Raman scattering configurations at the same probed spot.

Keywords: carbon nanotube, Raman spectroscopy, strain

(Some figures may appear in colour only in the online journal)

1. Introduction

Single-walled carbon nanotubes (SWCNTs) have been intensively studied for electronic device applications. Precise manipulation of the location and the alignment of SWCNTs is essential to making high quality electronic devices. In this context, vertically grown carbon nanotubes provide a new platform for fabricating high quality electronic devices. Recently, vertically grown single-walled carbon nanotubes (V-SWCNTs) have been used to make a field effect transistor [1], a solar cell [2], and thin film devices [3]. V-SWCNT forests have been successfully grown using various chemical vapor deposition (CVD) techniques, e.g. water-assisted CVD [4–6], alcohol-assisted CVD [7–12], oxygen-assisted plasma-enhanced CVD (PECVD) [13], molecular beam CVD [14], hot filament CVD methods [15], and microplasma-enhanced CVD [16]. Several Raman studies on V-SWCNT forests have recently been reported [5–14, 16]. Noticeably, Xiang *et al* confirmed, using resonance Raman spectroscopy, the successful synthesis of high quality ^{13}C-labeled V-SWCNT forests [10]. Polarized Raman studies on a V-SWCNT forest were used to find isolated SWCNTs suspended within the forest [11, 12]. Despite its importance, the existence of localized strains on V-SWCNTs has not been probed among several polarized Raman studies in the literature. In this work, localized strains in a V-SWCNT forest were studied using polarized micro-Raman spectroscopy.

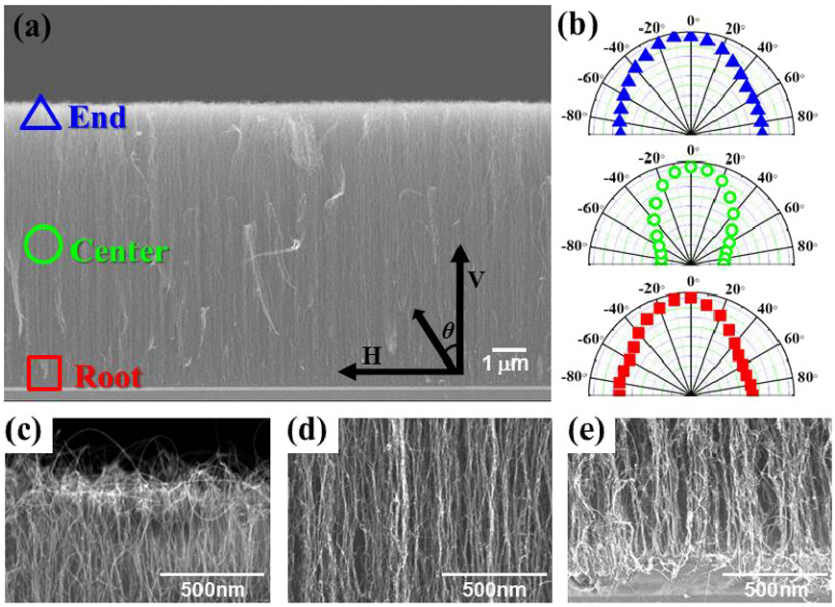

Figure 1. (a) SEM image of a vertically grown carbon nanotube forest; (b) polar plots of G-band Raman intensity, normalized with respect to that at $\theta = 0$, measured at the root, center, and end of the carbon nanotube forest. (c)–(e) Enlarged SEM images of the three different sections: (c) end, (d) center, and (e) root.

2. Experiments

Al thin film (10 nm) was deposited on a SiO_2 (200 nm)/Si substrate by thermal evaporation, and then oxidized at 600–700 °C in air to form an alumina supporting film for catalyst formation. An ultrathin iron film (∼0.5 nm) was deposited on the alumina-formed substrate and thermally oxidized at 600 °C for 10 min. V-SWCNTs were grown on the prepared substrate at 450 °C for 10 min using water-assisted PECVD [6, 17]. Raman spectra were obtained at room temperature using the 514.5 nm laser line from an Ar^+ laser as the excitation source. Incident light was focused onto the side of the V-SWCNT forest using a 60× objective lens. Scattered light was collected onto a spectrometer (Triax 552), whose focal length and spectral accuracy are 0.55 m and ∼1 cm^{-1}, respectively, and was detected with a liquid-nitrogen-cooled CCD detector.

3. Results and discussion

Figure 1(a) shows a scanning electron microscopy (SEM) image of a V-SWCNT forest, composed of ∼10 μm length carbon nanotubes, taken from a side of the forest. The H direction indicates a direction parallel to the substrate, and the V direction is parallel to the CNT growth direction, as shown in figure 1(a). In order to investigate the degree of CNT alignment, polarized Raman spectra were measured with VV and HH polarization configurations at the root (red square), center (green circle), and end (blue triangle) of the V-SWCNT forest. In the VV polarization configuration, the first V denotes the polarization direction of the incident light and the last V that of the scattered light. The polar plot of figure 1(b) shows the angular dependence of the normalized G-band Raman intensity with respect to that measured in the VV polarization configuration at $\theta = 0$. According to the polarized Raman selection rule for an isolated CNT, the G-band Raman intensity should be maximum in the VV polarization configuration ($\theta = 0$) and should vanish in the HH configuration ($\theta = 90$), if all the CNTs in the forest are perfectly aligned in the V direction. Thus, the relatively large Raman intensity ratio (I_{HH}/I_{VV}) at the root and the end of the CNT forest, as compared to that at the center, indicates that the degree of CNT alignment at the center was substantially higher than that at the root and the end of the forest [18, 19], which is clearly illustrated in figures 1(c)–(e), where the enlarged SEM images of the end, center, and root sections are shown.

RBM Raman spectra measured in the three different sections of the V-SWCNT forest are shown in figure 2(a), where two prominent peaks at 152 and 188 cm^{-1} were observed for the root and end sections, but the corresponding peaks for the center section were observed at 145 and 181 cm^{-1}. RBM Raman frequency (ω_{RBM}) is inversely proportional to the tube diameter (d_t), $\omega_{RBM} = 248/d_t$ [20]. It is worthwhile to note that diameter changes along the growth direction for V-SWCNT forests were reported, where the SWCNT diameter gradually increases from the end to the root due to the increase of the catalyst size through the Ostwald ripening or catalyst aggregation during the growth [21, 22]. If there were some diameter changes along the same ensemble of V-SWCNTs, suppression of the RBM features larger than ∼200 cm^{-1} and concurrent enhancement of the RBM features smaller than ∼140 cm^{-1} should have been observed as the probed spot moved from the end to the root section. We did not observe such changes that would indicate some diameter change along the growth direction in our RBM spectra. Any significant enhancement of lower frequency RBM features measured at the root section was not

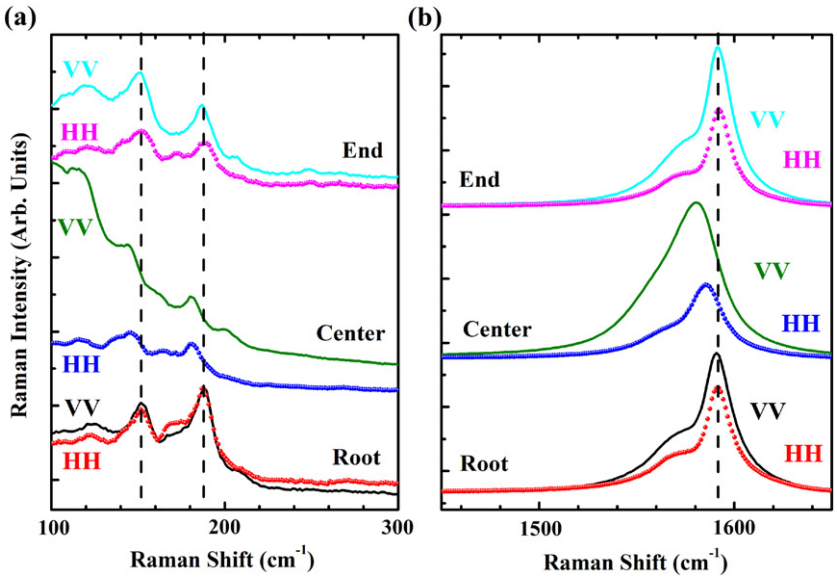

Figure 2. Normalized polarized Raman spectra of (a) RBM and (b) G-band, obtained in three different sections in the vertical grown single-walled carbon nanotube forest.

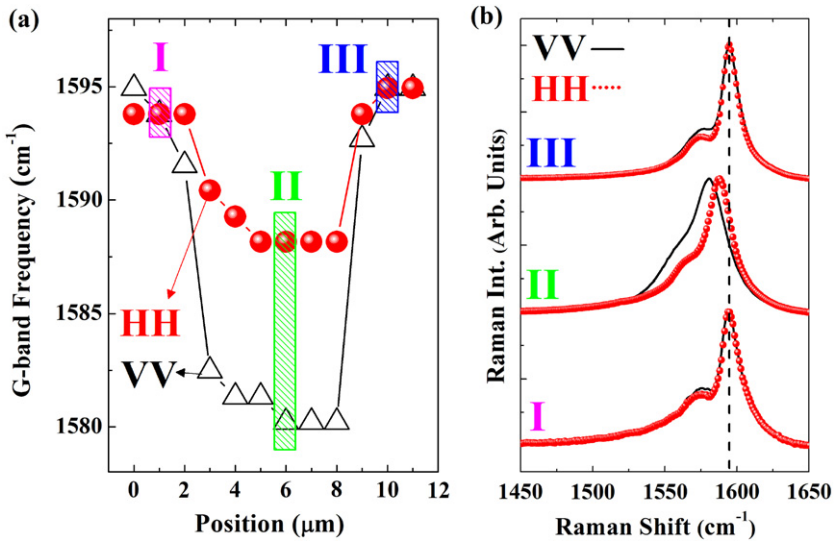

Figure 3. (a) G-band Raman frequencies measured at 12 different spots along the nanotube growth direction (V direction) in VV (black triangle) and HH (red solid circle) polarization configurations. (b) Normalized G-band Raman spectra measured at positions I, II, and III specified in (a).

observed, and the RBM spectra in the spectral range larger than ∼200 cm^{-1} were almost the same regardless of the probed spots. Thus, the observed RBM peak shift of 7 cm^{-1} for the center section cannot be attributed to a larger tube diameter in the center section as compared to the root and end sections. In this context, it is important to note that RBM Raman frequencies in bundled SWCNTs on a PDMS substrate downshifted when they were under strain [23]. The G-band Raman spectra, shown in figure 2(b), exhibit a prominent peak at 1592 cm^{-1} for the root and end sections but at 1580 cm^{-1} for the center section. Thus, Raman frequency downshifts of RBM and G-band were concurrently observed in the center section of the V-SWCNT forest. It is worth noting that the G-band Raman frequency at 1592 cm^{-1} is essentially diameter independent [20]. Thus, tube diameter fluctuations, if any, have no contribution to the observed G-band downshift in the center section of our samples.

Figure 3(a) shows G-band Raman frequencies measured at 12 different spots along the nanotube growth direction (V direction) in VV and HH polarization configurations. The G-band Raman frequencies measured at the root and end sections were ∼1594 cm^{-1} in both polarization configurations. However, the G-band Raman frequency measured in the center section downshifted by 5 or 13 cm^{-1} for HH or VV polarization configurations, respectively, with respect to that in the root section. Figure 3(b) shows the normalized Raman spectra for three different probed positions, labeled I, II, and III in figure 3(a), in VV and HH

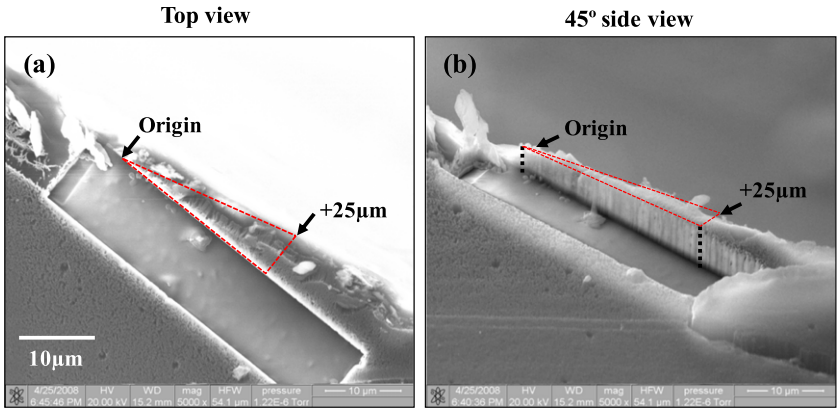

Figure 4. SEM images of a wedged vertical grown single-walled carbon nanotube forest: (a) top view (b) 45° side view. The excitation laser was incident on the side of the wedged vertical grown single-walled carbon nanotube forest at the center. The probed laser spot was moved from the thin part, labeled 'Origin', to the thicker one, labeled '+25 μm'.

configurations. It can be immediately noticed that the G-band Raman signature measured in the center section exhibits both frequency downshift and linewidth broadening with respect to that in the root and end sections. The G-band Raman frequency shift, reported in the literature, has been attributed to a change of temperature [11, 24], doping density [25, 26], or strain [27–31], but the frequency downshift and the concurrent linewidth broadening of the G-band, shown in figure 2, can only be ascribed to a strain [31]. Besides, the G-band Raman frequency measured in the center section exhibits strong polarization anisotropy, indicating a significantly larger strain in the V direction as compared to that in the H direction. The strain in the center section of our V-SWCNT forest, estimated from the G-band Raman frequency shift, is ∼0.8% [28]. As the SWCNTs grew, they were forced to bundle due to the van der Waals interaction between them, but the roots were anchored at the positions where the catalysts were located on the substrate, which should cause strain on the bundled section of the SWCNTs. Then, the bundled parts were likely to align in the growth direction whereas the end and the root sections have much less tendency to align in the growth direction. The end section is likely to be strain free because the SWCNTs are virtually 'free standing', and the root section is likely to be strain relaxed during the synthesis because the SWCNTs were synthesized last after the other upper sections were already bundled and strained. The SEM images in figures 1(c)–(e) seem to be consistent with our explanation for the occurrence of the alignment and the strain in our V-SWCNTs.

In order to investigate the effect of the thickness of the V-SWCNT forest on the strain observed in its center section, a wedged V-SWCNT forest was prepared near the boundary of the original forest by using the ion milling method. Figures 4(a) and (b) are the SEM images of the wedged V-SWCNT forest. The rectangular area in figure 4(a) is free of V-SWCNTs, that were removed by ion milling. Figure 4(b) shows that V-SWCNTs were still well aligned vertically after the ion milling. Polarized Raman spectra were measured by using the incident laser lights focused on the side of the wedged V-SWCNT forest at the center.

Figure 5(a) shows G-band Raman frequencies in VV and HH polarization configurations as a function of the probed position in the wedged V-SWCNT forest. The G-band Raman frequency of the thin parts of the wedged forest is ∼1590 cm^{-1} for both VV and HH configurations. However, in the rest of the wedged forest, the G-band Raman frequency exhibited a strong polarization anisotropy, ∼7 cm^{-1} difference between VV and HH configurations. In the VV polarization configuration, the G-band Raman frequency difference between the thin and the thick parts of the wedged forest was up to ∼14 cm^{-1}. Figure 5(b) shows the normalized G-band Raman spectra measured at two different probed positions, labeled I and II in figure 5(a), where the G-band Raman frequency shift and the concurrent polarization anisotropy for the thick part of the wedged V-SWCNT forest are clearly shown.

As for the origin of the strain in the V-SWCNTs, we think that the bundling of the individual SWCNTs during the growth played an important role. The bundling of SWCNTs occurs due to the van der Waals interaction between nearby SWCNTs, and the presence of water vapor around SWCNTs induces a substantially tighter bundling due to the hydrophobicity of their surface. The much lower growth temperature of 450 °C for our sample, as compared to that of 700–800 °C for other V-SWCNTs, may be responsible for the observed downshift of the G-band. It is likely that the bundling-induced strain could be relaxed more easily during the growth for higher growth temperature than for the much lowered growth temperature as adopted in our sample. Besides, our samples were grown by the water-plasma CVD method, which is different from the methods used in other V-SWCNTs. Very mild water plasma was used so that there were water vapors inside the growth chamber, which could have caused strong forces on the SWCNTs to tightly bundle as they grew, resulting in extra-tight bundling with substantial strain.

4. Conclusion

Our polarized micro-Raman study on a V-SWCNT forest revealed that the degree of V-SWCNT alignment was highest in the center section among three different sections (root, center, and end) along the vertical growth direction. The

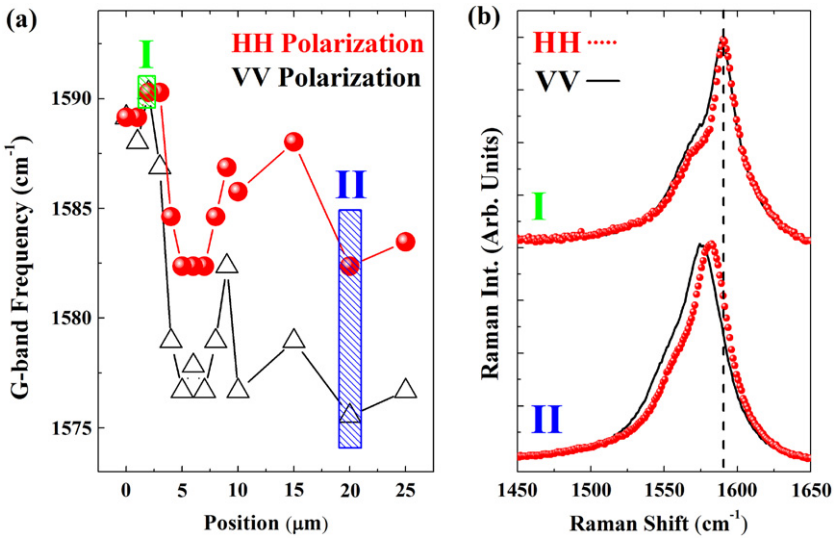

Figure 5. (a) G-band Raman frequencies in VV and HH polarization configurations as a function of the probed position in the wedged vertical grown single-walled carbon nanotube forest. (b) Normalized G-band Raman spectra measured at positions I and II.

observed Raman frequency red-shift of up to 13 cm^{-1} for the G-band in the center section, with respect to the Raman frequencies measured at the root and the end sections, and the concurrent linewidth broadening of the G-band in the center section, clearly indicate the existence of up to 0.8% strain localized in the center section. Strong polarization anisotropy of up to 8 cm^{-1} in the G-band Raman frequency in the center section indicates that the localized strain is predominantly in the vertical growth direction.

Acknowledgments

This research was supported by the Basic Science Research Program through the National Research Foundation of Korea (NRF) funded by the Ministry of Education, Science and Technology (2009-0093817, 2011-0010556, and 2013R1A1A2010595). SH acknowledges the support from the NRF (2009-0079103).

References

[1] Qu L, Du F and Dai L 2008 Preferential synthesis of semiconducting vertcally aligned single-walled carbon nanotubes for direct use in FETs *Nano Lett.* **8** 2682–7
[2] Chen J *et al* 2010 A quantum dot sensitized solar cell based on vertically aligned carbon nanotube templated ZnO arrays *Electrochem. Commun.* **12** 1432–5
[3] Im J *et al* 2009 Direct priting of aligned carbon nanotube patterns for high-performance thin film devices *Appl. Phys. Lett.* **94** 053109
[4] Hata K, Futaba D N, Mizuno K, Namai T, Yumura M and Iijima S 2004 Water-assited highly efficient synthesis of impurity-free single-walled carbon nanotubes *Science* **306** 1362–4
[5] Hasegawa K, Noda S, Sugime H, Kakehi K, Maruyama S and Yamaguchi Y 2008 Growth window and possible mechanism of millimeter-thick single-walled carbon nanotube forests *J. Nanosci. Nanotechnol.* **8** 6123–8
[6] Lee I H, Im J, Kim U J, Bae E J, Kim K, Lee E H, Lee Y H, Hong S and Min Y 2010 Low temperature growth of singe-walled carbon nanotube forest *Bull. Korean Chem. Soc.* **31** 2819–22
[7] Murakami Y, Chiashi S, Miyauchi Y, Hu M, Ogura M, Okubo T and Maruyama S 2004 Growth of vertically aligned single-walled carbon nanotube films on quartz substrates and their optical anisotropy *Chem. Phys. Lett.* **385** 298–303
[8] Noda S, Sugime H, Osawa T, Tsuji Y, Chiashi S, Murakami Y and Maruyama S 2006 A simple combinatorial method to discover Co–Mo binary catalysts that grow vertically aligned singel-walled carbon nanotubes *Carbon* **44** 1414–9
[9] Einarsson E, Kadowaki M, Ogura K, Okawa J, Xiang R, Zhang Z, Yamamoto T, Ikuhara Y and Maruyama S 2008 Growth mechanism and internal structure of vertically aligned single-walled carbon nanotubes *J. Nanosci. Nanotechnol.* **8** 6093–8
[10] Xiang R, Zhang Z, Ogura K, Okawa J, Einarsson E, Miyauchi Y, Shiomi J and Maruyama S 2008 Vertically aligned 13C single-walled carbon nanotubes synthesized by no-flow alcohol chemical vapor deposition and their root growth mechanism *Japan. J. Appl. Phys.* **47** 1971–4
[11] Murakami Y, Chiashi S, Einarsson E and Maruyama S 2005 Polarization dependence of resonant Raman scattering from vertically aligned single-walled carbon nanotube films *Phys. Rev.* B **71** 085403
[12] Zhang Z, Einarsson E, Murakami Y, Miyauchi Y and Maruyama S 2010 Polarization dependence of radial breathing mode peaks in resonant Raman spectra of vertically aligned single-walled carbon nanotubes *Phys. Rev.* B **81** 165442
[13] Zhang G *et al* 2005 Ultra-high-yield growth of vertical singel-walled carbon nanotubes: hidden roles of hydrogen and oxygen *Proc. Natl Acad. Sci.* **102** 16141–5
[14] Eres G, Kinkhabwala A A, Cui H, Geohegan D B, Puretzky A A and Lowndes D H 2005 Molecular beam-controlled nucleation and growth of vertically aligned single-wall carbon nanotube arrays *J. Phys. Chem.* B **109** 16684–94
[15] Xu Y, Flor E, Kim M J, Hamadani B, Schmidt H, Smalley R E and Hauge R H 2006 Vertical array growth of small diameter single-walled carbon nanotubes *J. Am. Chem. Soc.* **128** 6560–1
[16] Hiramatsu M, Deguchi T, Nagao H and Hori M 2007 Area-selective growth of aligned single-walled carbon

nanotube films using microwave plasma-enhanced CVD *Diamond Relat. Mater.* **16** 1126–30
[17] Min Y, Bae E J, Oh B S, Kang D and Park W 2005 Low-temperature growth of single-walled carbon nanotubes by water plasma chemical vaper deposition *J. Am. Chem. Soc.* **127** 12498–9
[18] Hwang J, Gommans H H, Ugawa A, Tashiro H, Haggenmueller R, Winey K I, Fischer J E, Tanner D B and Rinzler A G 2000 Polarized spectroscopy of aligned single-wall carbon nanotubes *Phys. Rev.* B **62** 310–3
[19] Duesberg G S, Loa I, Burghard M, Syassen K and Roth S 2000 Polarized Raman spectroscopy on isolated single-walled carbon nanotubes *Phys. Rev. Lett.* **85** 5436–9
[20] Dresselhaus M S, Dresselhaus G, Saito R and Jorio A 2005 Raman spectroscopy of carbon nanotubes *Phys. Rep.* **409** 47–99
[21] Xiang R, Einarsson E, Murakami Y, Shiomi J, Chiashi S, Tang Z and Maruyama S 2012 Diameter modulation of vertically aligned single-walled carbon nanotubes *ACS Nano* **6** 7472
[22] Chen Z, Kim D, Hasegawa K and Noda S 2013 Methane-assisted chemical vapor deposition yielding millimeter-tall single-wall carbon nanotubes of smaller diameter *ACS Nano* **7** 6719
[23] Kumar R, Aykol M and Cronin S B 2008 Effect of nanotube–nanotube coupling on the radial breathing mode of carbon nnaotubes *Phys. Rev.* B **78** 165428
[24] Zhang Y, Xie L, Zhang J, Wu Z and Liu Z 2007 Temperature coefficients of Raman frequency of individual single-walled carbon nanotubes *J. Phys. Chem.* C **111** 14031–4
[25] Das A, Sood A K, Govindaraj A, Saitta A M, Lazzeri M, Mauri F and Rao C N R 2007 Doping in carbon nanotubes probed by Raman and transport measurements *Phys. Rev. Lett.* **99** 136803
[26] Zhang L, Huang L, O'Brien S P and Yu Z 2008 Electrostatic doping-induced phonon shift of metallic single-wall carbon nanotubes *J. Phys. Chem.* C **112** 20118–22
[27] Cronin S B, Swan A K, Ünlü M S, Goldberg B B, Dresselhaus M S and Tinkham M 2004 Measuring the uniaxial strain of individual single-walled carbon nanotubes: resonance Raman spectra of atomic-force-microscope modified single-wall nanotubes *Phys. Rev. Lett.* **93** 167401
[28] Cronin S B, Swan A K, Ünlü M S, Goldberg B B, Dresselhaus M S and Tinkham M 2005 Resonant Raman sepctrosocpy of individual metallic and semiconducting single-wall carbon nanotubes under uniaxial strain *Phys. Rev.* B **72** 035425
[29] Son H, Samsonidze G G, Kong J, Zhang Y, Duan X, Zhang J, Liu Z and Dresselhaus M S 2007 Strain an dfriction induced by van der Waals interaction individual single walled carbon nanotubes *Appl. Phys. Lett.* **90** 253113
[30] Duan X, Son H, Gao B, Zhang J, Wu T, Samsonidze G G, Dresselhaus M S, Liu Z and Kong J 2007 Resonant Raman spectroscopy of individual strained single-wall carbon naotubes *Nano Lett.* **7** 2116–21
[31] Kumar R and Cronin S B 2007 Raman scattering of carbon nanotube bundles under axial strain and strain-induced debundling *Phys. Rev.* B **75** 155421